PACS numbers: **42.25.–p**, **42.62.–b**, 42.65.Re
DOI: 10.3367/UFNe.0185.201501h.0097

Subterawatt femtosecond pulses in the mid-infrared range: new spatiotemporal dynamics of high-power electromagnetic fields

A V Mitrofanov, D A Sidorov-Biryukov, A A Voronin, A Pugžlys, G Andriukaitis, E A Stepanov, S Ališauskas, T Flöry, A B Fedotov, V Ya Panchenko, A Baltuška, A M Zheltikov

Abstract. **Subterawatt ultrashort pulses in the mid-infrared (mid-IR) range delivered by a multistage optical parametric chirped pulse amplifier are used to study laser-induced filamentation and optical-harmonic generation in the field of a mid-IR driver. Conditions and physical scenarios enabling filamentation-assisted compression of subterawatt mid-IR pulses to few-cycle pulse widths are identified.**

Keywords: ultrashort laser pulses, self-focusing, laser filamentation, mid-infrared radiation

1. Introduction

Understanding the new physics behind the interaction of powerful ultrashort pulses of electromagnetic radiation in the mid-infrared (mid-IR) range with matter is one of the main challenges in modern optical science. Intense studies performed within the past few years have provided new important insights into the key mechanisms whereby ultrashort pulses of electromagnetic radiation interact with different materials, helping to reveal the main properties of the optical response of matter to high-power ultrashort mid-IR pulses [1–3] and predict new physical effects and unusual regimes of ultrafast processes [2–5] occurring in the presence of high-power low-frequency electromagnetic fields.

While laser sources of high-power ultrashort pulses in the near-infrared range benefit from remarkably efficient laser material with a gain band sufficient for the generation of few-cycle pulses, such materials are lacking in the mid-IR range, making it difficult to extend ultrafast laser technologies into this spectral range. Within the past two or three years, it has been demonstrated, however, that highly efficient sources of ultrashort pulses in the mid-IR range can be created using nonlinear-optical parametric frequency conversion of ultrashort pulses. The technology of optical parametric chirped pulse amplification (OPCPA) has been shown recently to enable the generation of ultrashort laser pulses with a central wavelength of around 4 μm [6] and energy up to 10 mJ. Laser sources of this class made it possible to perform the first experimental studies of high-order optical nonlinearities in the atmosphere and rare gases [7, 8] and demonstrate high-order harmonic generation, yielding coherent X-rays with a photon energy up to 1.3 keV [9]. The peak power provided by OPCPA mid-IR sources of ultrashort pulses was sufficient for beam filamentation in high-pressure gases [8, 10], leading to the first observation of lasing in a filament [11] within the second positive band of molecular nitrogen. Supported by theoretical studies [4, 12], these experiments suggest the existence of new forms of light–matter interaction occurring in the mid-IR range. For the experimental observation of these forms, however, the existing cutting-edge sources of ultrashort pulses in the mid-IR range need to be upgraded to the subterawatt level of peak powers.

In this study, OPCPA technology is implemented with a 1-J picosecond laser pump to produce sub-100-fs mid-IR pulses with a peak power above 0.3 TW. Experiments performed with this source of ultrashort pulses in the mid-IR range demonstrate that ultrashort mid-IR pulses with an energy above 20 mJ can be transmitted through the atmosphere in the single-filament mode. Experimental studies presented below in this paper reveal new forms of optical harmonic generation and help to identify physical scenarios enabling filamentation-assisted compression of subterawatt mid-IR pulses to widths of only a few optical cycles.

2. Generation of subterawatt femtosecond pulses in the mid-infrared range

High-power ultrashort pulses of mid-IR radiation were produced using the laser system (Figs 1 and 2) consisting of a solid-state ytterbium master oscillator with a regenerative amplifier, an intermediate three-stage optical parametric amplifier, and a three-stage optical parametric chirped-pulse amplifier. A solid-state $Yb{:}CaF_2$ master oscillator [6] delivered ultrashort pulses with a central wavelength of around 1030 nm. Taking advantage of a regenerative amplification of the master-oscillator output [13] yielded sub-200-fs pulses with an energy up to 15 mJ and a pulse repetition rate of 1 kHz [14]. The amplified sub-200-fs output of the ytterbium front-end system with an energy ranging from 3 to 12 mJ was utilized in near-infrared filamentation experiments presented below in this paper.

Ultrashort pulses in the mid-IR range were produced through two cascades of optical parametric amplification.

A V Mitrofanov Lomonosov Moscow State University, Moscow, Russian Federation;
Russian Quantum Center, Skolkovo, Moscow region, Russian Federation;
Institute of Laser and Information Technologies, Russian Academy of Sciences, Shatura, Moscow region, Russian Federation;
National Research Centre 'Kurchatov Institute', Moscow, Russian Federation
D A Sidorov-Biryukov, A A Voronin, E A Stepanov, A B Fedotov Lomonosov Moscow State University, Moscow, Russian Federation;
Russian Quantum Center, Skolkovo, Moscow region, Russian Federation
A Pugžlys, G Andriukaitis, S Ališauskas, T Flöry, A Baltuška Vienna University of Technology, Vienna, Austria
V Ya Panchenko Institute of Laser and Information Technologies, Russian Academy of Sciences, Shatura, Moscow region, Russian Federation;
National Research Centre 'Kurchatov Institute', Moscow, Russian Federation
A M Zheltikov Lomonosov Moscow State University, Moscow, Russian Federation;
Russian Quantum Center, Skolkovo, Moscow region, Russian Federation;
National Research Centre 'Kurchatov Institute', Moscow, Russian Federation;
Texas A&M University, College Station, TX, USA
E-mail: zheltikov@physics.msu.ru

Uspekhi Fizicheskikh Nauk **185** (1) 97–103 (2015)
DOI: 10.3367/UFNr.0185.201501h.0097
Translated by A M Zheltikov; edited by A Radzig

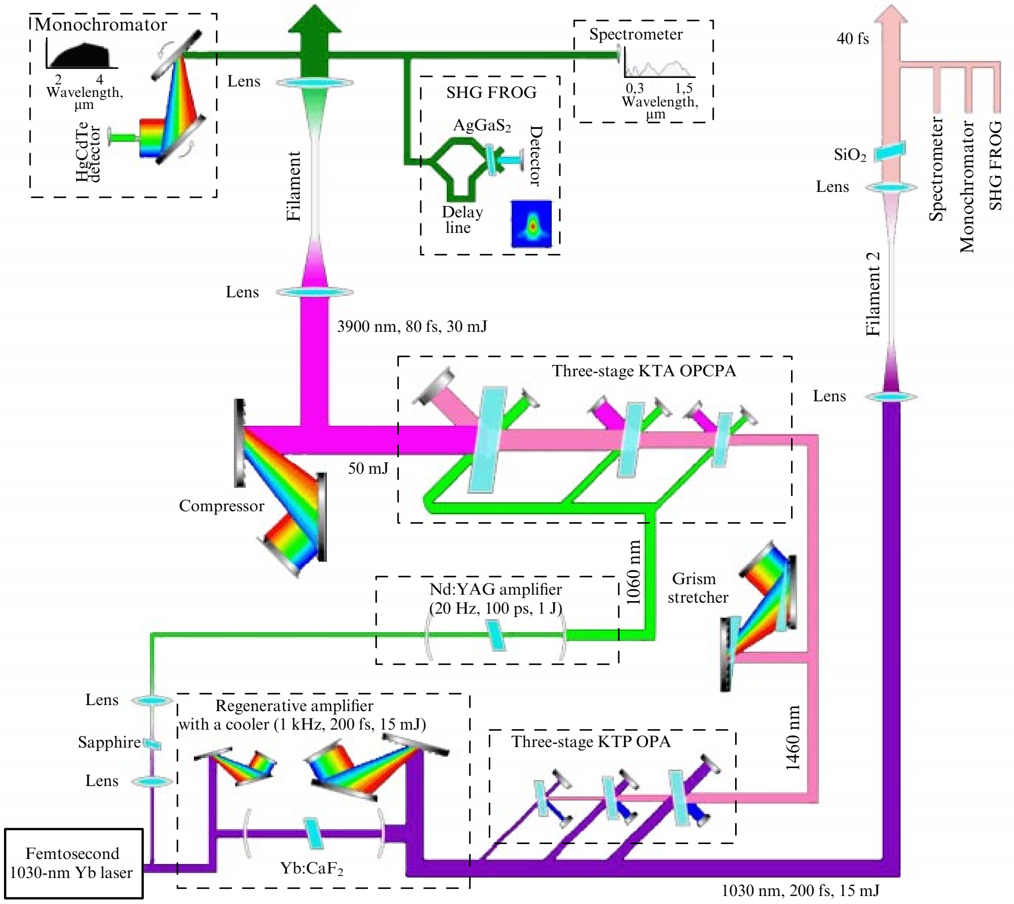

Figure 1. Layout of a source of high-power ultrashort pulses in the mid-infrared range, consisting of a solid-state ytterbium front-end laser, an intermediate three-stage optical parametric amplifier, and a mid-infrared three-stage optical parametric chirped pulse amplifier.

In the first cascade, the regeneratively amplified output of the ytterbium front-end laser system with a central wavelength of 1030 nm, energy of about 1 mJ, and a pulse length of about 190 fs were used as a pump in a three-stage setup of optical parametric amplification (Fig. 1), yielding pulses with a pulse width of about 200 fs centered at around 1460 nm at the output of this setup. These pulses were then stretched with a grism stretcher to be utilized as a seed for a signal wave in three-stage optical parametric chirped-pulse amplification, implemented using a series of three KTA ($KTiOAsO_4$) nonlinear-optical crystals. To pump these three crystals, a three-beam 100-ps output from an Nd:YAG laser with energies of 50, 250, and 750 mJ was used. The energy of the idler-wave output of the OPCPA system exceeded 50 mJ. Following compression of these pulses with making use of a grating compressor, mid-IR pulses with an energy up to 30 mJ and a pulse width ranging from 80 to 200 fs were produced at a central wavelength of 3.9 μm.

Spectral measurements in the mid-IR range were performed with a homemade scanning monochromator and a thermoelectrically cooled HgCdTe detector. Standard Ocean Optics spectrometers were exploited for spectral measurements in the visible and near-IR ranges. Temporal pulse characterization with a phase retrieval was performed by means of frequency-resolved optical gating (FROG) based on second-harmonic generation in a 0.5-mm thick $AgGaS_2$ crystal.

The dashed line with shading in Fig. 3 displays a typical spectrum of a high-power idler-wave OPCPA output. A FROG trace of this pulse is presented in Fig. 4a. The temporal envelope and the phase of this pulse, retrieved from this FROG trace, are shown in Fig. 4b.

3. Laser filamentation in the mid-infrared range

The implemented OPCPA technology promotes mid-IR ultrafast optics to a qualitatively new level. The OPCPA system described in the previous section allows laser peak powers sufficient for laser filamentation in the atmosphere to be achieved for the first time in the mid-IR range. A laser filament can be induced in a medium with a Kerr-nonlinearity coefficient n_2 and a refractive index n_0, when the peak power of an ultrashort laser pulse is markedly higher than the critical power of self-focusing, $P_{cr} = C(8\pi n_0 n_2)^{-1}\lambda^2$, where λ is the radiation wavelength, and C is a beam-lateral-profile-dependent numerical factor ($3.72 < C < 6.4$). In earlier gas-phase experiments, laser filamentation in the mid-IR range was only possible in gases with a pressure of several atmospheres. The peak power provided by laser sources available for earlier studies was not sufficient to induce laser filaments at atmospheric pressure.

In our experiments, laser filamentation in the atmosphere becomes possible due to the high peak power of mid-IR ultrashort laser pulses provided by the OPCPA-based source. Our experimental studies demonstrate that ultrashort pulses

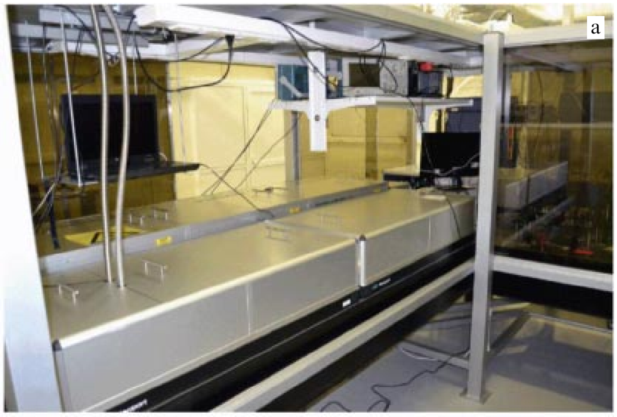

Figure 2. Laser source of subterawatt ultrashort pulses in the mid-infrared range. Photographs taken at the Advanced Photonics Laboratory of the Russian Quantum Center.

of electromagnetic radiation with a central wavelength of 3.9 μm, a pulse width of 80–130 fs, and a peak power of about 0.2–0.3 TW can produce filaments in the atmosphere. When loosely focused with a custom-made calcium fluoride lens, such pulses give rise to an extended spark, clearly indicating efficient ionization of the atmospheric air, accompanied by a dramatic spectral broadening of the mid-IR pulse (see Fig. 3).

Filamentation of mid-IR pulses in the atmosphere was observed in our experiments within a broad range of focal lengths f of the lens employed to focus the mid-IR beam. With the peak power and the pulse width of the mid-IR driver

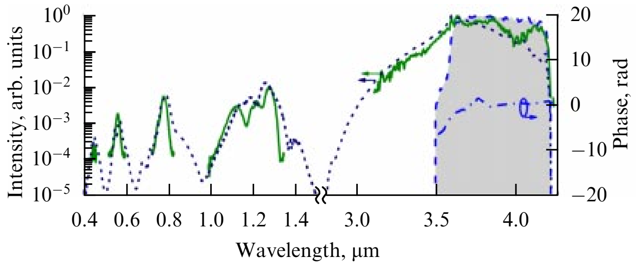

Figure 3. Spectrum (dashed line with shading) and the spectral phase (dashed–dotted line) of the idler-wave OPCPA output, shown against the experimental (solid line) and simulated (dotted line) spectra of radiation at the output of the filament induced by pulses with a central wavelength of 3.9 μm, a pulse width of 90 fs, and an energy of 22 mJ focused by a lens with a focal length of 75 cm in the atmosphere.

fixed, the specific value of this focal length controls the maximum field intensity and the electron number density inside a filament (Fig. 5). Laser filamentation in the mid-IR range was simulated applying the model of short-pulse evolution in the mid-IR range, constructed in earlier studies [7, 8, 10]. This modeling shows that, as the focal length of the focusing lens is increased from 45 to 200 cm, the maximum electron density in the filament lowers by more than an order of magnitude (Fig. 5a), while the extent of the ionized gas increases from a few centimeters to 1.5 m.

Similar tendencies are observed for the longitudinal profile of field intensity (Fig. 5b). As the focal length of the focusing lens grows from 45 to 200 cm, the maximum field intensity in the filament decreases from 46 to 30 TW cm^{-2}. The length of the region where the field intensity is clamped near its maximum level, indicating a well-formed filament, increases, reaching 1.5 m with $f = 200$ cm.

4. Spectral evolution of subterawatt pulses in the mid-infrared range: high-power mid-infrared supercontinuum and optical-harmonic generation

Filamentation of ultrashort pulses in the mid-IR range is accompanied by several new effects that are not observed in filaments induced by near-infrared laser pulses. It is therefore instructive to compare the physical scenario of filamentation in the mid-IR range with thoroughly understood scenarios of laser filamentation in the near-infrared range [15–17]. To this end, we present in Figs 6 and 7 the results of numerical

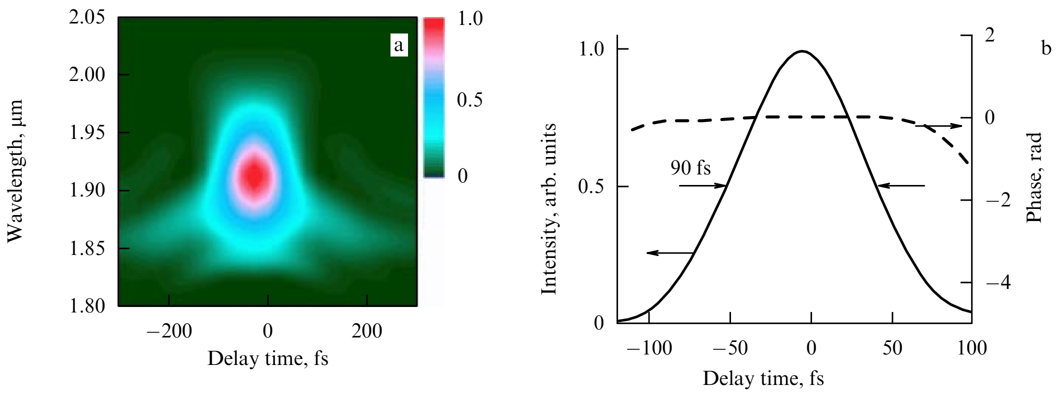

Figure 4. (a) FROG trace of the idler-wave OPCPA output, and (b) the temporal envelope and the phase retrieved from this trace.

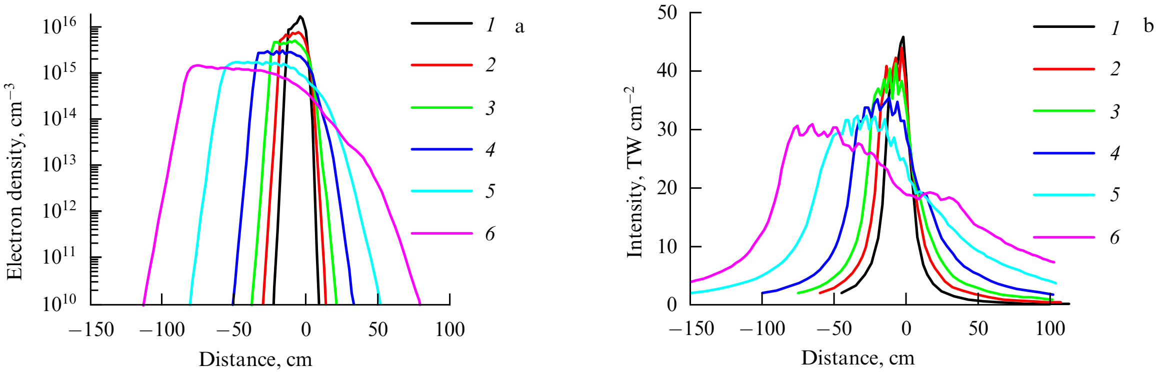

Figure 5. (Color online.) Dynamics of (a) the electron density on the trailing edge of the pulse, and (b) the maximum field intensity on the beam axis in a filament induced by pulses with a central wavelength of 3.9 μm, a pulse width of 100 fs, and an energy of 20 mJ in the atmosphere. The driver beam is focused by a lens with a focal length of 45 cm (*1*), 60 cm (*2*), 75 cm (*3*), 100 cm (*4*), 150 cm (*5*), and 200 cm (*6*).

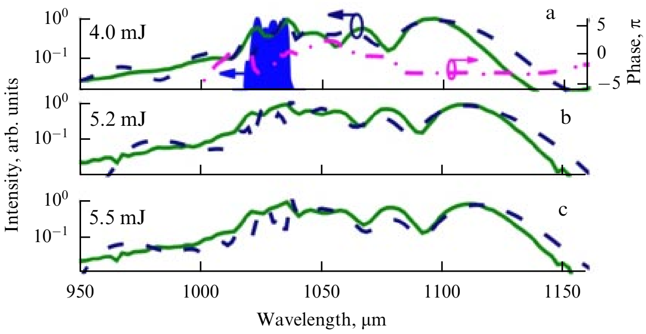

Figure 6. Spectra of supercontinuum radiation from a filament induced by a regeneratively amplified ytterbium-laser output in the atmosphere. The central wavelength of the driver is 1030 nm, the driver pulse width is 200 fs, and the driver energy is 4.0 mJ (a), 5.2 mJ (b), and 5.5 mJ (c). The spectrum of the driver is shown by shading. The solid curve depicts the experimental results. The dashed curve presents the results of numerical simulations. The dashed–dotted curve demonstrates the spectral phase retrieved from FROG measurements.

simulations performed for laser filaments induced by the near-infrared output of an ytterbium regenerative amplifier (see Fig. 1) with a central wavelength of 1030 nm, a pulse width of about 200 fs, and an energy ranging within 4–10 mJ.

Similar to laser filamentation in the mid-IR range, filamentation of near-infrared pulses gives rise to a dramatic spectral broadening of laser pulses (see Fig. 6). This effect is due to nonlinear-optical interactions enhanced through the suppression of diffraction-induced divergence of the laser beam within extended regions inside a laser filament. However, the spectral broadening of 3.9-μm pulses in the long-wavelength spectral region is limited by molecular absorption bands of the atmosphere. As a result, the long-wavelength part of the supercontinuum, which is especially intense for high-energy near-infrared pulses (see Fig. 6), is strongly suppressed for the supercontinua emitted from mid-IR filaments (see Fig. 3).

Unlike its long-wavelength wing, the high-frequency part of the supercontinuum output of a mid-IR filament is enhanced by efficient optical-harmonic generation (see Fig. 3). A weak dispersion of the atmospheric air in the mid-IR range improves phase matching for a group of low-order

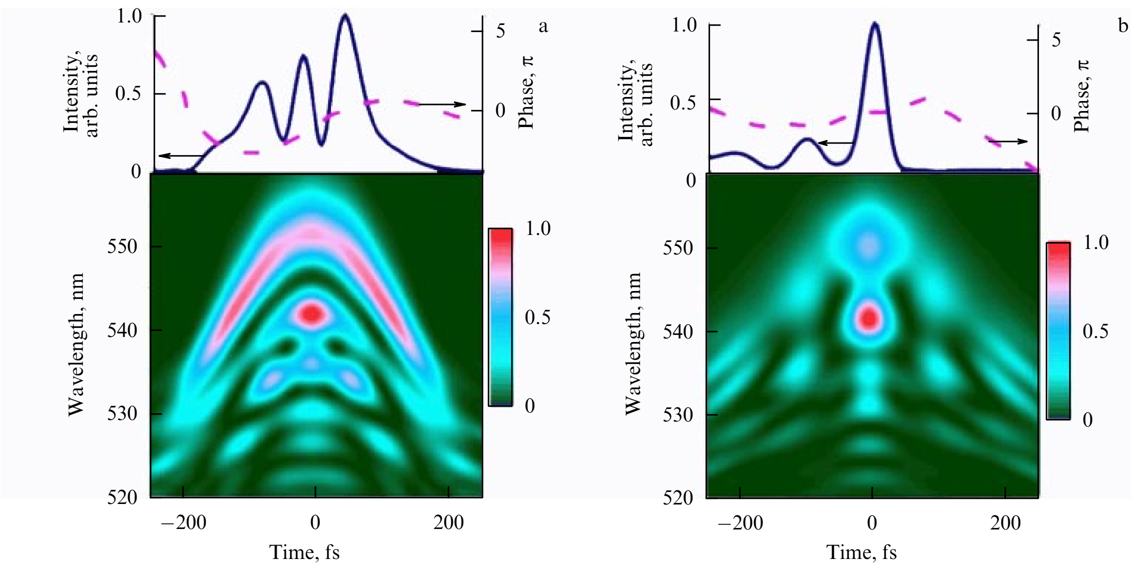

Figure 7. (Color online.) FROG traces for (a) the filament output, and (b) the filament output compressed in a 6-cm thick fused silica slab. The central wavelength of the driver is 1030 nm. The driver energy reaches 4 mJ. Temporal envelopes and phase profiles retrieved from the FROG traces are shown on top.

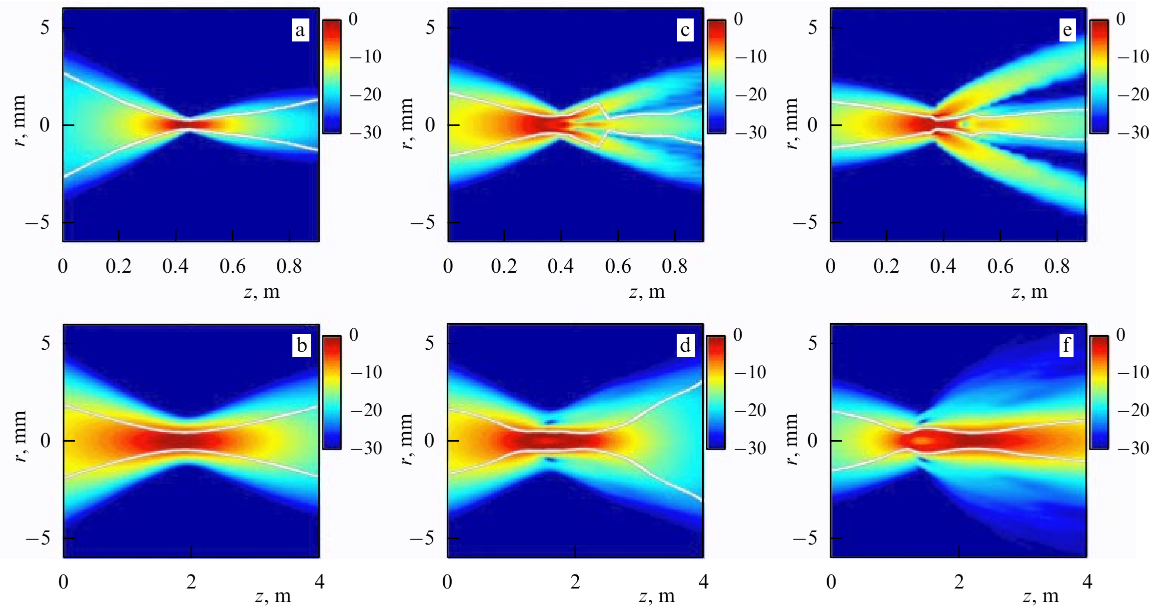

Figure 8. Spatiotemporal maps of field intensity in a subterawatt ultrashort mid-IR pulse propagating in the atmosphere (a, b) at the leading edge, (c, d) in the central part, and (e, f) at the trailing edge of the pulse. The beam is focused by a lens with a focal length of 45 cm (a, c, e) and 200 cm (b, d, f). The initial driver energy is 20 mJ. The initial pulse length of the driver is 100 fs. The solid line marks the full width at half-maximum beam diameter.

optical harmonics, thus enhancing harmonic generation relative to harmonic generation by a near-infrared driver. Moreover, a whole group of low-order optical harmonics of the mid-IR driver used in our experiments, including its third, fifth, seventh, and ninth harmonics, falls within the transparency region of atmospheric air, thus leading to a further enhancement of the harmonic signal.

A theoretical analysis fully verifies the enhancement of optical harmonic generation in a filament induced by a mid-IR driver due to the suppression of diffraction divergence of the driver beam, increasing the extent of interaction between the pump field and its harmonics and maintaining a high pump intensity within this interaction domain. Intense peaks representing optical harmonics in the spectrum of supercontinuum radiation generated by a mid-IR filament are noticeably broadened (see Fig. 3) due to cross-phase modulation and blue-shifted due to the strong scattering of the driver off the fast-ionizing gas [15, 18].

5. Spatiotemporal dynamics of subterawatt ultrashort mid-infrared pulses in the atmosphere

To gain deeper insights into the physical scenario of the ultrashort pulse filamentation in the mid-IR range, we plot in Fig. 8 maps of field intensity distributions in the filament calculated for the leading edge (Figs 8a and 8b), the central part (Figs 8c and 8d), and the trailing edge (Figs 8e and 8f) of the pulse. As can be seen from these simulated results, different sections of the beam undergo different dynamics with the electron density increasing from the leading edge of the pulse to its trailing edge. The leading edge of the pulse originates ionization of the air, giving rise to a transverse profile of the electron density, falling off from the center of the beam to its periphery. Such a profile of the electron density defocuses the central part and, especially, the trailing edge of the pulse. These dynamics are clearly seen in the maps of a field intensity presented in Fig. 8. The scattering of mid-IR radiation off the field-induced plasma also becomes especially strong in the trailing edge of the pulse, leading, in the case of long filaments (curve *6* in Fig. 5b), to noticeable pump depletion along a filament.

The white solid line in Fig. 8 depicts the beam diameter d defined as the beam full width at half-maximum (FWHM) of the field intensity. The evolution of the beam diameter d along the optical path of the mid-IR driver provides a convenient measure of the filament length as the distance between two points along the beam path, where the beam diameter is equal to twice the minimum beam diameter within a filament. When the beam focusing is too tight (Figs 8a, 8c, and 8e), strong scattering of the central part (Fig. 8c) and the trailing edge (Fig. 8e) of the pulse from the electron-density profile induced by the leading edge of the pulse limits the length of the filament. An appropriate choice of beam-focusing conditions (Figs 8b, 8d, and 8f) can help to achieve a precise balance between beam self-focusing and defocusing at the transverse profile of the electron density. In this regime, the filament length, as can be seen from Fig. 8f, can reach several meters, offering unique options for remote sensing of the atmosphere and long-range transmission of high-power laser pulses.

6. Compression of high-power ultrashort mid-infrared pulses

Efficient spectral broadening of intense ultrashort pulses, enhanced by beam filamentation, offers a powerful technology for pulse compression, thus enabling the generation of ultrahigh-power electromagnetic field waveforms as short as a few light field cycles. Filamentation-based compression of high-power light pulses in the near-infrared range is widely tapped in modern optical technologies. Those regimes that would enable filamentation-assisted compression of mid-IR pulses are still to be identified.

The difference in physical scenarios and mechanisms behind the spectral broadening of ultrashort pulses in near- and mid-infrared filaments suggests that filamentation-based

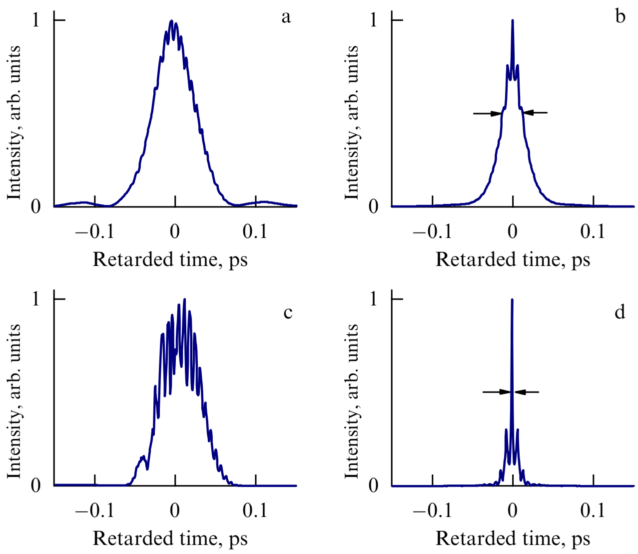

Figure 9. (a) Temporal envelope of the broadband radiation at the output of a filament induced by driver pulses with a central wavelength of 3.9 μm, a pulse width of 90 fs, and a peak power of about 0.3 TW. (b) The transform-limited pulse supported by the entire spectrum of the broadband filament output. (c) Temporal envelope of the filament output behind a filter blocking wavelengths longer than 2 μm. (d) The transform-limited pulse behind the spectral filter.

approaches to pulse compression and a few-cycle waveform synthesis in the near- and mid-infrared ranges should also be distinct. Experimental and theoretical studies give evidence (Figs 6 and 7) that broadband field waveforms generated in near-infrared filaments can be efficiently compressed through a compensation of phase distortions using optical components with a properly chosen dispersion and a carefully optimized length. Figure 7 gives experimental results demonstrating that the filamentation-assisted spectral broadening enables compression of laser pulses with a central wavelength of 1030 nm and an initial pulse width of 200 fs to a pulse width of about 40 fs through compensation of phase distortions in a 6-cm thick slab of fused silica.

Laser filamentation in the mid-IR range suggests new approaches to pulse compression due to a radical enhancement of the short-wavelength part of supercontinua emitted by mid-IR filaments, provided by efficient optical-harmonic generation in such filaments (see Fig. 3). Temporal compression of such a broadband waveform is difficult to implement in practice, as it requires an accurate compensation of phase shifts within a bandwidth of several octaves. One possible solution to this problem may involve spectrally decomposing this broadband waveform within several bands and parallel compensation of phase shifts within each of these bands, followed by a coherent combining of these components, which is aimed at synthesizing an extremely short field waveform. In Fig. 9a, we plot the temporal envelope of the broadband output of a filament generated by driver pulses with a central wavelength of 3.9 μm, a pulse width of 90 fs, and a peak power of 0.3 TW. The FWHM transform-limited pulse width supported by the entire spectrum of this waveform (Fig. 9b) equals 27 fs. This transform-limited pulse consists of an extremely short pulse carrying the field of optical harmonics, and a pedestal produced by the long-wavelength part of the supercontinuum. A spectral filter that blocks the long-wavelength part of the supercontinuum spectrum helps to separate the short harmonic pulse from the long pedestal, giving rise to a pulse with a temporal envelope shown in Fig. 9c. A transform-limited pulse that can be produced through an ideal compensation of phase distortions, following such a spectral filtering, has a pulse width of about 2 fs (Fig. 9d), which approximately corresponds to half the light field cycle at the central wavelength (1.1 μm) of the spectrally filtered field waveform.

7. Conclusion

Generation of sub-100-fs mid-IR pulses with a peak power above 0.3 TW is demonstrated using optical parametric chirped-pulse amplification technology with a 1-J picosecond laser pump. Experiments performed with the employment of this source of ultrashort pulses in the mid-IR range demonstrate that ultrashort mid-IR pulses with an energy above 20 mJ can be transmitted through the atmosphere in the regime of a single filament. Experimental research presented in this work reveals new forms of optical harmonic generation and suggests physical scenarios enabling filamentation-assisted compression of subterawatt mid-IR pulses to widths of only a few optical cycles.

Acknowledgments
This research was supported in part by the Russian Foundation for Basic Research (project Nos 13-02-01465, 13-02-92115, 14-02-00784, and 14-29-07182) and the Welch Foundation (grant No. A-1801). Research on ultrafast nonlinear optics in the mid-infrared range was supported by the Russian Science Foundation (project No. 14-12-00772). A A V gratefully acknowledges the support of his research by the Dynasty Foundation.

References

1. Colosimo P et al. *Nature Phys.* **4** 386 (2008)
2. Agostini P, DiMauro L F *Contemp. Phys.* **49** 179 (2008)
3. Shiner A D et al. *Phys. Rev. Lett.* **103** 073902 (2009)
4. Serebryannikov E E, Zheltikov A M *Phys. Rev. Lett.* **113** 043901 (2014)
5. Voronin A A, Zheltikov A M *Phys. Rev. A* **90** 043807 (2014)
6. Andriukaitis G et al. *Opt. Lett.* **36** 2755 (2011)
7. Kartashov D et al. *Opt. Lett.* **37** 2268 (2012)
8. Kartashov D et al. *Opt. Lett.* **37** 3456 (2012)
9. Popmintchev T et al. *Science* **336** 1287 (2012)
10. Kartashov D et al. *Opt. Lett.* **38** 3194 (2013)
11. Kartashov D et al. *Phys. Rev. A* **86** 033831 (2012)
12. Bergé L *Opt. Express* **16** 21529 (2008)
13. Pugžlys A et al. *Opt. Lett.* **34** 2075 (2009)
14. Mitrofanov A V et al. *Opt. Lett.* **39** 4659 (2014)
15. Bergé L et al. *Rep. Prog. Phys.* **70** 1633 (2007)
16. Zheltikov A M *Phys. Usp.* **49** 605 (2006); *Usp. Fiz. Nauk* **176** 623 (2006)
17. Zheltikov A M *Phys. Usp.* **54** 29 (2011); *Usp. Fiz. Nauk* **181** 33 (2011)
18. Zheltikov A M, Koroteev N I *Phys. Usp.* **42** 321 (1999); *Usp. Fiz. Nauk* **169** 385 (1999)